Corticostriatal synaptic function in mouse models of Huntington's disease: early effects of huntingtin repeat length and protein load

Austen J. Milnerwood[1,2] and Lynn A. Raymond[1,2]

[1]*Department of Psychiatry,* [2]*Brain Research Centre, University of British Columbia, Vancouver, Canada V6T 1Z3*

Huntington's disease (HD) is an autosomal dominant, late onset, neurodegenerative disease characterized by motor deficits and dementia that is caused by expansion of a CAG repeat in the HD gene. Clinical manifestations result from selective neuronal degeneration of predominantly GABAergic striatal medium-sized spiny neurons (MSNs). A growing number of studies demonstrate that personality, mood and cognitive disturbances are some of the earliest signs of HD and may reflect synaptic dysfunction prior to neuronal loss. Previous studies in striatal MSNs demonstrated early alterations in NMDA-type glutamate receptor currents in several HD mouse models, as well as evidence for presynaptic dysfunction prior to disease manifestations in the R6/2 HD fragment mouse model. We have compared corticostriatal synaptic function in full-length, human HD gene-carrying YAC transgenic mice expressing a non-pathogenic CAG repeat (YAC18; control) with three increasingly severe variants of pathogenic HD gene-expressing mice (YAC72 and two different lines of YAC128), at ages that precede any detectable disease phenotype. We report presynaptic dysfunction and a propensity towards synaptic depression in YAC72 and YAC128 compared to YAC18 mice, and, in the most severe model, we also observed altered AMPA receptor function. When normalized to evoked AMPAR currents, postsynaptic NMDAR currents are augmented in all three pathogenic HD YAC variants. These findings demonstrate multiple perturbations to corticostriatal synaptic function in HD mice, furthering our understanding of the early effects of the HD mutation that may contribute to cognitive dysfunction, mood disorders and later development of more serious dysfunction. Furthermore, this study provides a set of neurophysiological sequelae against which to test and compare other mouse models and potential therapies in HD.

(Received 4 August 2007; accepted after revision 15 October 2007; first published online 18 October 2007)
Corresponding author A. J. Milnerwood: Deptartment of Psychiatry, University of British Columbia, 2255 Wesbrook Mall, Vancouver, Canada V6T 1Z3. Email: amilnerwood@gmail.com

Huntington's disease (HD) is an autosomal dominant, neurodegenerative disease. The HD gene includes a CAG repeat (HDCRG, 1993) encoding a polyglutamine tract (polyQ) in the protein huntingtin (htt). Repeat length > 35 is inversely correlated with age of HD onset, and juvenile onset generally occurs with > 70 repeats (Duyao *et al.* 1993). HD is characterized by disorders of movement, mood and cognition associated with prominent degeneration of GABAergic medium-sized spiny neurones (MSNs) in the striatum, which receive glutamatergic input from all cortical areas (Vonsattel *et al.* 1985).

The ubiquitously expressed htt protein is involved in protein and organelle transport (DiFiglia *et al.* 1995). Mutant huntingtin (mhtt) is expressed, and appears to localize, similarly to the normal protein (Aronin *et al.* 1995; Landwehrmeyer *et al.* 1995), and biochemical studies indicate it interferes with axonal transport and alters presynaptic vesicle release (Li *et al.* 2001; Gunawardena *et al.* 2003; Szebenyi *et al.* 2003; Trushina *et al.* 2004). Additionally, enhanced activity of NMDA-type glutamate receptors (NMDARs) which can kill neurons by excitotoxicity (reviewed in Beal, 1992; Choi, 1992), in MSNs may contribute to HD pathology (reviewed in Yohrling & Cha, 2002; Fan & Raymond, 2007). However, NMDARs also play a critical role in activity-dependent neuronal signalling, including synaptic plasticity, gene transcription, and cell survival (reviewed in Bliss & Collingridge, 1993; Pláteník *et al.* 2000; Hardingham, 2006).

Notably, recent evidence suggests neuronal dysfunction occurs prior to manifest disease in humans and mouse

 DOI: 10.1113/jphysiol.2007.142448

models (Usdin *et al.* 1999; Lawrence *et al.* 2000; Berrios *et al.* 2002; Li *et al.* 2004; Mazarakis *et al.* 2005; Cummings *et al.* 2006; Milnerwood *et al.* 2006*a*; Paulsen *et al.* 2006*b*; Cummings *et al.* 2007; Duff *et al.* 2007; Solomon *et al.* 2007). Some of the earliest changes in HD mice include altered NMDAR-dependent plasticity (Usdin *et al.* 1999; Murphy *et al.* 2000; Milnerwood *et al.* 2006*a*; Lynch *et al.* 2007), augmented NMDAR current (Levine *et al.* 1999; Cepeda *et al.* 2001; Li *et al.* 2004; Starling *et al.* 2005; Andre *et al.* 2006; Fan *et al.* 2007) and increased sensitivity to NMDAR toxicity (Zeron *et al.* 2001, 2002, 2004; Shehadeh *et al.* 2006). Additionally, altered glutamate release at the corticostriatal synapse develops just before motor signs in the R6/2 HD fragment model (Cepeda *et al.* 2003). Thus, early perturbations of NMDAR signalling, as well as glutamate release, at the corticostriatal synapse may be responsible for initial cognitive and emotional disturbances (Paulsen *et al.* 2006*a*), in addition to driving more severe pathological changes over time.

We have demonstrated specifically increased synaptic NMDAR current in YAC72 HD mouse MSNs relative to wild-type (WT) controls (Li *et al.* 2004). However, expression of exogenous full-length htt may in itself have effects, regardless of the mutation. Moreover, it is of interest to determine if similar changes, and possibly additional synaptic dysfunction, are observed in more severe HD models. Therefore, we recorded corticostriatal transmission in acute slices from yeast artificial chromosome (YAC) HD mice (Hodgson *et al.* 1999; Slow *et al.* 2003; Graham *et al.* 2006). These animals express full-length human htt, with polyQ corresponding to: (i) non-pathogenic (YAC18), (ii) high (YAC72), and (iii) very high (YAC128) repeat lengths. Additionally, we compared low (line 55) and high (line 53) htt-expressing variants of the YAC128 model. Recordings were made 1 month prior to detection of cognitive dysfunction in the most severe model, YAC128(53) (Van Raamsdonk *et al.* 2005), and prior to detection of motor deficits in any genotype, which are first seen at 2.5 and 7 months for YAC128(53) and YAC72, respectively (Hodgson *et al.* 1999; Van Raamsdonk *et al.* 2005; Graham *et al.* 2006). Our findings confirm previous studies indicating mhtt increases NMDAR current relative to that mediated by AMPARs. Additionally, we observed presynaptic dysfunction and, in the most severe model, YAC128(53), AMPAR current alterations in mhtt-expressing mouse corticostriatal synapses.

Methods

Transgenic mice and brain slice preparation

Transgenic YAC18, YAC72 (line 2511), YAC128 (line 55) and YAC128 (line 53) mice (Hodgson *et al.* 1999; Slow *et al.* 2003), expressing full-length human huntingtin containing 18, 72 or 128 CAG repeats were bred on an FVB/N background at the UBC Medicine Animal Resource Unit, and maintained according to Canadian Council on Animal Care regulations. All experiments were conducted on mice aged between postnatal days 21 and 30 (26.1 mean ± S.E.M. 0.3 days). To eliminate possible bias introduced by postnatal age, care was taken to ensure that mean age was $26 \pm < 1$ in all groups, and that there were no significant age differences ($P > 0.8$) between genotypes. Acute corticostriatal slices were prepared: in accordance with the UBC Animal Care Committee and the Canadian Council on Animal Care, to minimize suffering mice were killed by decapitation following deep halothane vapour anaesthesia. The brain was rapidly removed and immersed in oxygenated (95% O_2–5% CO_2), chilled ($\sim +4^{\circ}$C) artificial cerebrospinal fluid (ACSF, containing (mM): 125 NaCl, 2.5 KCl, 25 $NaHCO_3$, 1.25 NaH_2PO_4, 2 $MgCl_2$, 2 $CaCl_2$, 25 glucose, pH 7.3–7.4, 300–310 mosmol l^{-1}). Coronal slices 300 μm thick were cut on a vibratome (Leica VT1000) and placed in a holding chamber containing ACSF at room temperature (RT) for > 1 h prior to recording. Slices were transferred to a submersion recording chamber, on a DIC-IR microscope (Axioskop, Zeiss), and held in a known orientation with a standard harp. The chamber was continuously perfused ($\sim$2 ml min^{-1}) with oxygenated ACSF + 100 μM picrotoxin (PTX, Tocris Bioscience, MO, USA) at RT. Slices were left to equilibrate for $\sim$20 min prior to electrophysiological recording.

Electrophysiology

Cells were visualized using a water-immersion objective lens (Achroplan ×60) attached to a video camera and monitor. MSNs were identified by somatic size (8–20 μm), morphology and location, with target cells located in the centre of caudate putamen (CPu) at $\sim$50–150 μm beneath the slice surface. Data were acquired with a MultiClamp 700A amplifier and Clampex10 software interfaced to a Digidata 1322A acquisition board. Signals were filtered at 2 kHz, digitized at 10 kHz and analysed in Clampfit10 (Axon Instruments, CA, USA). Whole cell patch-clamp recording was performed in voltage clamp mode. Pipette resistance (R_p) was 3–6 MΩ (mean 5.4 ± 0.04 MΩ) when filled with solution containing (mM): 130 caesium methanesulphonate, 5 CsCl, 4 NaCl, 1 $MgCl_2$, 5 EGTA, 10 Hepes, 5 QX-314, 0.5 GTP, 10 Na_2-phosphocreatine, and 5 MgATP, pH 7.3, 280–290 mosmol l^{-1}. Series resistances (R_s) were < 25 MΩ (mean 16.9 ± 0.65 MΩ) and uncompensated; experiments were discontinued and rejected if R_s changed by $> 25\%$ (mean change, $\Delta R_s = 3.65 \pm 2.3\%$). There were no significant differences in R_p, R_s or ΔR_s between genotypes. Initial membrane properties were assessed soon after whole-cell (WC) configuration, with hyperpolarizing voltage steps (10 mV)

and the integrated membrane test function in Clampex10, which reports membrane capacitance, input resistance and time constants (a further measure for MSN identification). Recording stability and R_s were regularly monitored in this way, in addition to hyperpolarizing deflections (10 mV) and manual off-line calculation of membrane properties within each evoked current trace. Cell viability was assessed first by the smooth surface of the somatic membrane, as well as by the presence of fast sodium (typically > 2000 pA, first occurring at approximately -50 mV) and slow, delayed calcium (> 500 pA, first occurring at approximately -20 mV) currents within a passive current–voltage relationship (*I–V*), produced by a series of depolarizing voltage steps (holding potential V_h -70 mV, 500 ms, -60 to 0 mV, 0.066 Hz), which were recorded soon after establishing WC configuration ($\sim$1 min, prior to complete intracellular perfusion of the use-dependent sodium channel blocker QX-314). These values are typical of MSNs when Cs-based internal solution is used (C. Cepeda, personal communication).

Recordings were made in the presence of 100 μM PTX to block $GABA_A$-mediated inhibition, with the further bath application of 10 μM 6-cyano-2,3-dihydroxy-7-nitro-quinoxaline (CNQX) or 50 μM D-(–)-2-amino-5-phosphonopentanoic acid (D-AP5) where stated (Tocris Bioscience, MO, USA). Spontaneous postsynaptic EPSCs (sEPSCs) were isolated and analysed using the Clampfit10 event analysis function with a detection threshold set at 8 pA (typically 2–3 times root mean square noise). All events were checked by eye with experimenter blind to genotype, and events with non-unitary baseline, peak or decay were suppressed from all analysis other than mean cell frequency (Hz). For kinetic analysis events were aligned and averaged for each cell, and genotype cell means were compared. For amplitude and interevent interval cumulative probability plots, all isolated sEPSCs were included from 2 min continuous recording periods, commencing 2–3 min after establishment of WC configuration and following passive *I–V*. Individual cell cumulative probability plots were constructed and genotype mean $\pm$ S.E.M. are shown. For analysis of sEPSC occurrence frequency by amplitude bin, the number of cells analysed per genotype were randomly reduced to match the smallest group, in order to eliminate any bias in the absolute number of occurrences. Additionally, for this analysis (but not others) the number of events per cell was limited to the first 100, yielding 800–1000 events per genotype. EPSCs were also evoked (eEPSCs) by intra-striatal electrical stimulation (200 μs, 10–800 μA) of cortical afferent fibres via a glass micropipette filled with ACSF (2–5 MΩ) placed 150–200 μm dorsally toward the corpus callosum. For some pharmacological experiments concomitant field recording was performed; field electrodes were the same as patch electrodes (but filled with ACSF) and were placed at the same tissue depth within 50–100 μM of the target cell. Evoked AMPA and NMDA receptor-mediated currents were averages of at least three evoked responses (evoked at 0.066 Hz) and kinetics were assessed by single and double exponential fits and reported as τ or τ weighted (τ_W), respectively ($\tau_W = [I_f/(I_f + I_s)]\tau_f + [I_s/(I_f + I_s)]\tau_s$, where τ_f = tau fast, τ_s = tau slow), as previously described (Stocca & Vicini, 1998). For NMDA : AMPA ratios AMPA currents were recorded at $V_h = -70$ mV, cells then held at +60 mV, CNQX (10 μM) added to the perfusate, and responses evoked at 0.016 Hz to track AMPA receptor blockade. After 5 min, CNQX had abolished all AMPAR current, leaving only NMDAR-mediated current, as evidenced by the ablation of the field potential and slowing of the eEPSC rise time. Results are mean $\pm$ S.E.M. Statistical significance was tested by one-way and non-repeated measures two-way ANOVA and direct comparison by Student's *t* test (unless stated otherwise) with Kruskal–Wallis and Welch corrections where stated using Prism (Graphpad Software, CA, USA) and Excel (Microsoft Corp., CA, USA).

Results

AMPA receptor-mediated spontaneous excitatory postsynaptic currents

Putatively healthy MSNs in the central area of the CPu were identified by somatic morphology and size, and stimulating and recording electrodes were placed under high power ($\times$60) visual guidance. In the presence of the $GABA_A$ antagonist picrotoxin (100 μM), spontaneous activity recorded from striatal MSNs (clamped at -70 mV) is the result of glutamate release and consequent AMPA receptor (AMPAR)-mediated current. Spontaneous EPSCs (sEPSCs) recorded in this manner are a mixed sample of action potential-mediated and miniature EPSCs (mEPSCs); of these, we find that the majority ($\sim$80%) are mEPSCs, in agreement with others (Wu N *et al.* 2007). Traditionally, the frequency of mEPSCs is regarded as indicative of presynaptic release probability (P_r), and thus presynaptic release efficacy (Thomson, 2000; reviewed in Sudhof, 2004; Zucker, 2005), whereas mEPSC kinetics are thought to reflect postsynaptic AMPAR subunit composition. Although mEPSC amplitude is generally taken to be representative of postsynaptic AMPAR numbers (reviewed in Lisman, 2003), a recent study reported quantal size (mEPSC amplitude) varies predominantly as a function of vesicular glutamate concentration (Wu XS *et al.* 2007).

Analysis of sEPSCs in MSNs is shown in Fig. 1. Despite a trend towards lower frequency in YAC128 MSNs, one-way ANOVA demonstrated no significant effects of genotype ($P = 0.7$, $F_{3,66} = 0.5$) upon mean cell frequency (Fig. 1*B*).

However, it was noted that the maximum frequency observed in YAC128(55) and YAC128(53) cells was 3.82 and 3.90 Hz, respectively, whereas 22 and 27% of YAC18 and YAC72 cells, respectively, had mean frequencies above the observed YAC128 maximum. Mean cell interevent intervals (IEIs) were also not significantly different by ANOVA, but there were highly significant differences in the variance of both YAC128 group IEIs, with respect to YAC18 (F test, $P < 0.003$). Two-way ANOVA of mean IEI cumulative probabilities also demonstrated no significant effect of genotype; however, whilst YAC18 and YAC72 cumulative probability plots were indistinguishable, there was a strong trend towards longer intervals between sEPSC events in YAC128(53) MSNs (Fig. 1*C*, for clarity data shown only for YAC18 and YAC128(53)). The YAC128(55) IEI plot lay between those of YAC18 (and

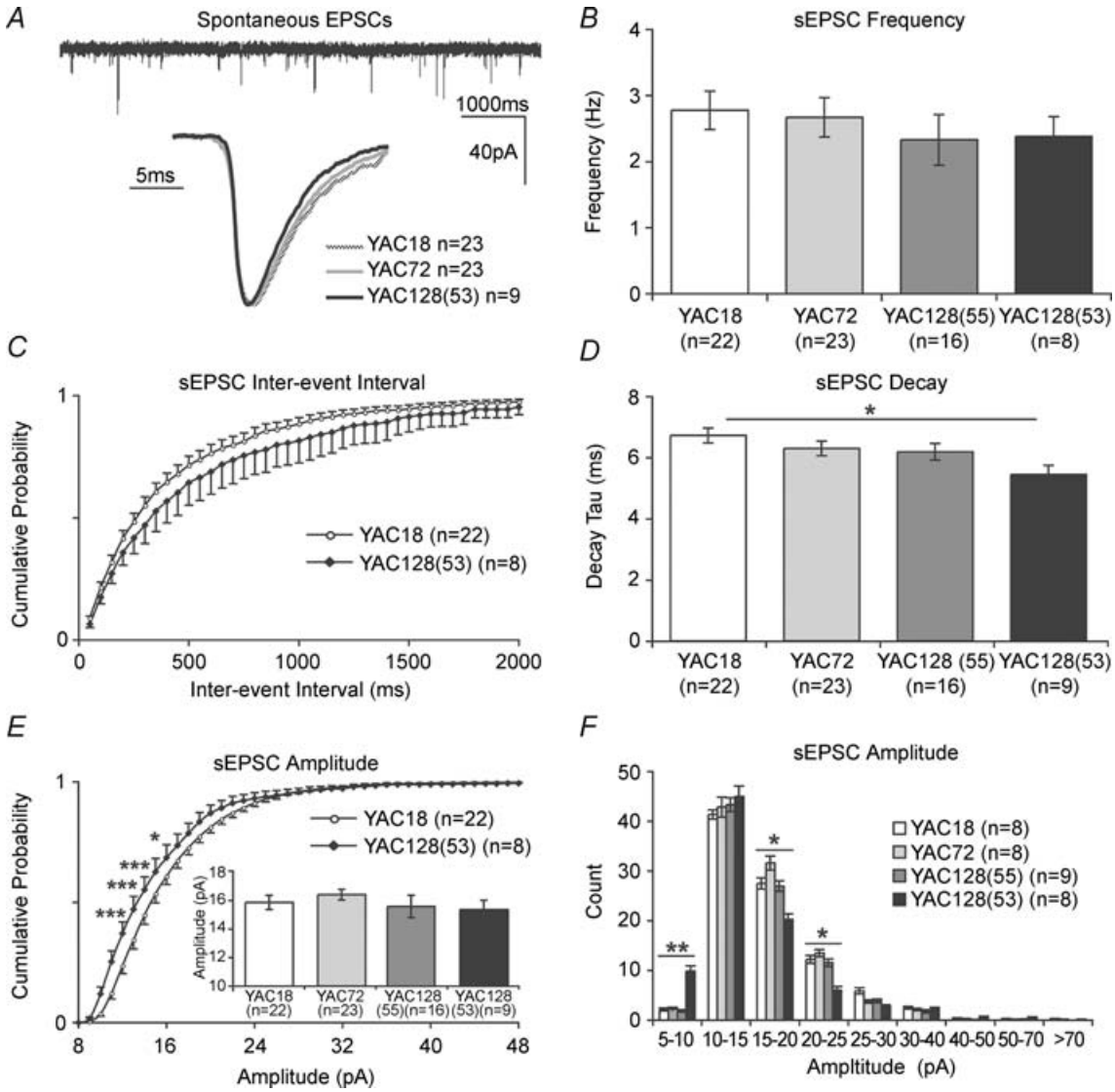

Figure 1. Spontaneous glutamatergic transmission and AMPAR function
A: top, a typical example of AMPAR-mediated spontaneous EPSCs (sEPSCs) obtained by WC recording of striatal MSNs in the absence of $GABA_A$ transmission (100 μM PTX, V_h −70 mV, YAC18); bottom, average peak-scaled events, for clarity only three genotypes are shown. *B*, sEPSC mean cell frequencies are not significantly altered across genotypes. *C*, sEPSC interevent intervals were also not significantly different, although a trend is apparent, in YAC128(53) MSNs with respect to YAC18. *D*, sEPSC decay kinetics are significantly faster in YAC128(53) MSNs than YAC18 (also see *A*). *E*, sEPSC mean cell amplitudes are not significantly different between genotypes (inset), whereas mean YAC128(53) sEPSC amplitude cumulative probability plots demonstrate a significantly higher proportion of smaller events with respect to YAC18. *F*, sEPSC amplitude bins similarly demonstrate a higher frequency of smaller AMPAR-mediated events, in addition to a lower frequency of medium-sized events in YAC128(53) MSNs with respect to YAC18. $^*P < 0.05$, $^{**}P < 0.01$, $^{***}P < 0.001$.

YAC72) and YAC128(53). Together the data suggest that in the most severe models mhtt expression results in subtle alterations in P_r that may reflect presynaptic dysfunction. Alternatively, differences in the number of functional synapses may contribute to the subtle alterations in event frequency.

For kinetic analysis, events were isolated and an average cell event produced (average sEPSCs shown in Fig. 1*A*). Analyses of genotype means were then conducted on these cell averages. As shown in Fig. 1*D*, there is a polyglutamine length-dependent trend towards faster decay kinetics. One-way ANOVA demonstrated a significant effect of genotype ($P < 0.04$, $F_{3,67} = 3.10$) upon sEPSC decay; direct comparisons revealed that mean AMPAR current decay was significantly faster in YAC128(53) than in YAC18 MSNs (YAC18, 6.59 ± 0.23 ms, $n = 23$; YAC128(53), 5.34 ± 0.29 ms, $n = 9$, $P < 0.02$). The data indicate that the expression of mhtt results in alterations to AMPAR function and/or subunit composition, which manifests as faster decay kinetics.

Differences were also observed between YAC18 and YAC128(53) MSNs in AMPAR sEPSC amplitude distributions (Fig. 1*E* and *F*), although one-way ANOVA demonstrated no significant effect of genotype upon the cell mean event amplitudes (Fig. 1*E*, inset, $P > 0.7$). Mean cell cumulative probability plots for all sEPSC amplitudes, shown in Fig. 1*E*, demonstrated a significant interaction between genotype and amplitude ($P < 0.0001$, $F_{129,2795} = 1.914$ by two-way ANOVA). Bonferroini *post hoc* analysis revealed the distribution of amplitudes to be significantly different i.e. generally smaller YAC128(53) sEPSCs, as demonstrated by higher cumulative fractions in the 11, 12, 13 ($P < 0.001$) and 14 pA ($P < 0.05$) range than YAC18 sEPSCs. Cumulative probability plots for YAC18 and YAC72 sEPSCs were indistinguishable, while the YAC128(55) plot lay between that of YAC18 and YAC128(53) (for clarity not shown in Fig. 1*E*). In order to further investigate the relative frequencies of different-sized events, limited event numbers (see Methods) from individual cells were separated into amplitude bins to create a genotype mean ± S.E.M. across the spectrum of amplitudes (Fig. 1*F*). Statistical comparisons were made between pairs of genotypes for all bins using two-way ANOVA. By this analysis there were no significant differences between YAC18 and YAC72 or YAC128(55) event amplitude bins, but there was a significant interaction between genotype and amplitude ($P < 0.006$, $F_{8,126} = 2.9$) for YAC18 and YAC128(53). sEPSC counts were significantly higher in YAC128(53) than YAC18 MSNs in the 5–10 pA amplitude range (YAC18, 2.125 ± 0.3, $n = 8$; YAC128(53) 9.88 ± 1.03, $n = 8$, $P < 0.01$ by *t* test). There were also significantly less frequent medium-sized events in YAC128(53) MSNs, relative to YAC18 in the 15–20 (YAC18, 27.5 ± 1.1, $n = 8$; YAC128(53) 20.25 ± 1.14, $n = 8$, $P < 0.05$) and 20–25 pA amplitude bins (YAC18, 12.25 ± 0.8, $n = 8$; YAC128(53) 6.25 ± 1.03, $n = 8$, $P < 0.02$). Thus, whilst the mean cell amplitude of sEPSCs in the modal range (10–15 pA) is not significantly different between genotypes, the distribution around the mode is significantly altered in YAC128(53) MSNs.

Taken together, analyses of sEPSCs demonstrate that presynaptic release is subtly perturbed and that AMPAR subunit composition and/or number is altered in the most severe model (YAC128(53)). Similar changes may have begun to occur in the YAC128 model with lower HD transgene expression (line 55), although any differences are apparent only as trends at this age. On the other hand, no differences in sEPSC amplitudes or frequencies were apparent between YAC18 and YAC72 MSNs, suggesting P_r for spontaneous glutamate release is not greatly affected and that postsynaptic AMPAR numbers are equivalent. Importantly, there were no significant differences between genotypes in the occurrence of larger (> 40 pA) sEPSCs (Fig. 1*F*), arguing that the increased proportion of smaller sEPSCs in YAC128(53) cells is not simply attributable to loss of larger (presumably action potential-dependent) spontaneous currents, due to reduced cortical cell firing.

eEPSC paired-pulse facilitation

To further investigate whether presynaptic release efficacy is altered at mhtt-expressing corticostriatal synapses, we turned to stimulus-evoked synaptic current. An increase or decrease in the relative amplitude of an evoked EPSC (eEPSC) that is the second of two stimulus-evoked pulses (separated by tens, or a few hundreds, of milliseconds; referred to as paired pulses) is believed to be indicative of presynaptic release probability (Zucker, 1973) with low paired-pulse facilitation ratio reflecting a high (initial) probability of presynaptic release (P_r) and vice versa. As shown in Fig. 2, at an interstimulus interval of 100 ms (150 μA stimulation intensity) the paired-pulse ratio of YAC18 corticostriatal synapses is mildly facilitatory ($7.8 \pm 2.1\%$ greater than initial, $n = 23$). One-way ANOVA of paired-pulse facilitation (PPF) ratios demonstrated a significant effect of genotype ($P < 0.03$, $F_{3,70} = 3.3$); direct comparisons revealed that PPF was significantly greater in YAC72, YAC128(55) and YAC128(53) synapses, relative to YAC18 (YAC72 $14.9 \pm 2.7\%$, $n = 26$, $P < 0.03$; YAC128(55) $15.5 \pm 4.5\%$, $n = 14$, $P < 0.05$; and YAC128(55) $24.1 \pm 5.6\%$, $n = 8$, $P < 0.001$). The data demonstrate an early deficit in evoked glutamate release at the corticostriatal synapse in all expanded mhtt-expressing mice, with the greatest change occurring in the most severe model (YAC128(53)).

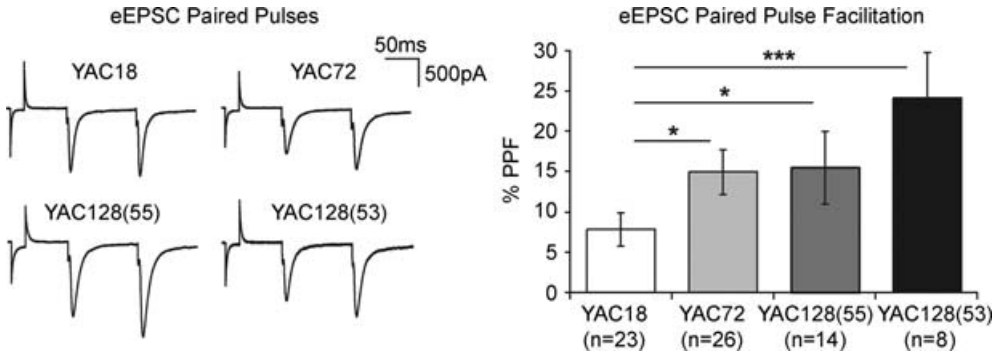

Figure 2. Altered paired-pulse facilitation (PPF)
Left, representative examples (traces are averages of 3 sweeps). Pairing two evoked EPSCs (interstimulus interval 100 ms) results in facilitation of the second response. Right: the degree of facilitation is significantly greater at all three mhtt-expressing mouse corticostriatal synapses, suggesting decreased probability of initial presynaptic release (*$P < 0.05$, ***$P < 0.001$).

Evoked NMDA and AMPA receptor-mediated excitatory postsynaptic currents

Initial experiments, designed to assess full input/output curves for evoked AMPAR- and NMDAR-mediated currents, suggested that activity-dependent reduction of evoked currents had occurred. Furthermore, the extent of this reduction appeared to be genotype dependent. In order to investigate this, currents were evoked (50–150 μA, −70 mV) at 0.1 Hz for 10 min (Fig. 3*A*).

This pattern of synaptic activity resulted in a small but significant ($P < 0.05$) decrease in YAC18 peak current amplitude over time (Fig. 3*B*, last 5 shocks compared to first 5; $-4.92 \pm 3.2\%$). Significant reductions ($P < 0.001$) were also observed in YAC72 and YAC128(53) MSNs ($-14.18 \pm 3.5\%$ and $-25.99 \pm 6.6\%$, $n = 6$ and 3, respectively). One-way ANOVA demonstrated a significant effect of genotype ($P < 0.02$, $F_{2,11} = 7.14$); direct comparisons revealed that the reductions observed in YAC72 and YAC128(53) currents were significantly greater than those observed in YAC18 ($P < 0.05$ and $P < 0.01$, respectively). This appeared to occur after ∼6 min of stimulation (after 30–50 shocks since commencement of WC recording). In light of this observation, in all subsequent experiments the number of stimuli was minimized (∼20); consequently only two stimulation intensities were investigated (50 and 150 μA; corresponding to approximately 30 and 80% of maximum eEPSC, respectively).

MSNs were held at −70 mV, and responses were evoked at the two stimulus intensities. At this holding voltage the vast majority of current generated in response to afferent stimulation is AMPAR-mediated, as evidenced by ablation of current and loss of field potential in the presence (< 5 min) of the AMPAR antagonist CNXQ (not shown). AMPAR eEPSC peak amplitudes are shown in Fig. 4*A*. Two-way ANOVA demonstrated a significant

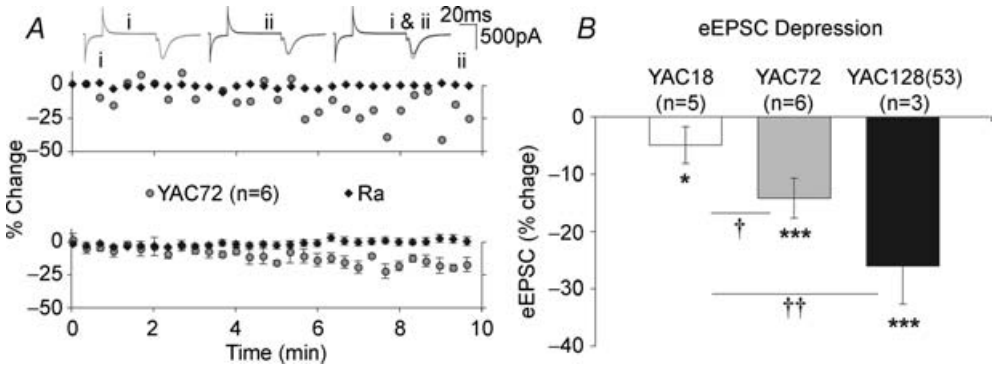

Figure 3. Reduction of evoked current magnitude is elevated in mhtt-expressing MSNs
A, 10 min of afferent stimulation resulted in a reduction in the amplitude of eEPSCs over time. Representative example (top) and grouped data (bottom) demonstrating that YAC72 MSN AMPAR-mediated current (V_h −70 mV) reduced with repetitive stimulation, in the absence of any alteration to access resistance (R_a). *B*, these reductions were significant (*$P < 0.05$, ***$P < 0.001$) in YAC18 MSNs (although modest) and both YAC72 and YAC128(53) MSNs. eEPSC amplitude reductions were significantly greater in YAC72 and YAC128(53) MSNs than those in YAC18 MSNs (†$P < 0.05$, ††$P < 0.01$).

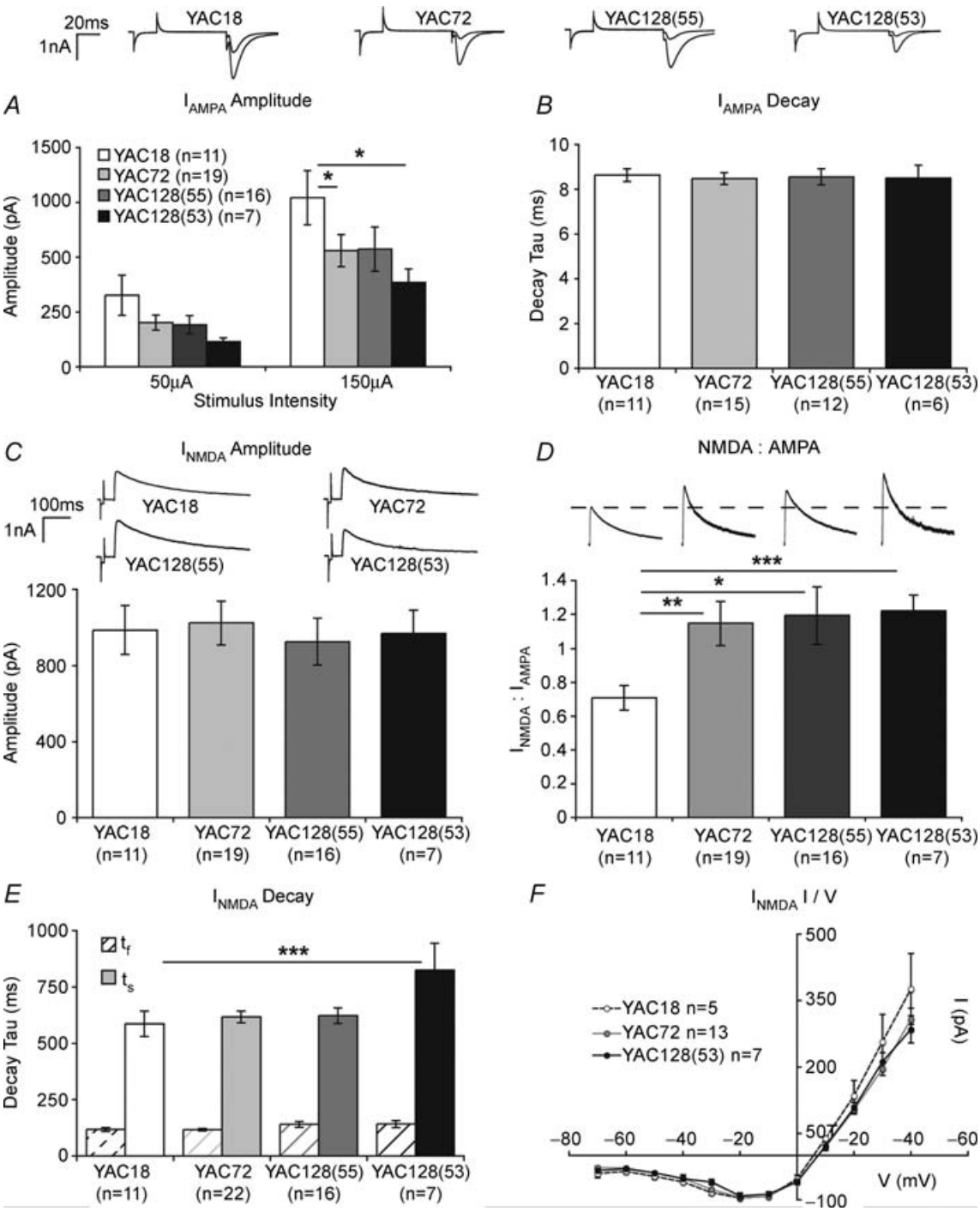

Figure 4. Stimulus-evoked currents and altered NMDAR transmission in mhtt-expressing MSNs
Representative traces of predominantly AMPAR-mediated eEPSCs (I_{AMPA}) produced by 50 and 150 μA stimulation in YAC mice are shown (top, averages of 3 sweeps V_h −70 mV). *A*, at near-maximal stimulation, AMPAR-mediated eEPSC amplitudes are significantly reduced in YAC72 and YAC128(53) MSNs. *B*, eEPSC AMPAR current decay kinetics are not significantly different across genotypes. *C*, isolated NMDAR eEPSC amplitudes are similar across genotypes (inset, same cells as shown for I_{AMPA}, V_h +60 mV, 10 μM CNQX). *D*, the ratio of isolated NMDAR eEPSC peak amplitude to AMPAR eEPSC peak amplitude is significantly higher in all mhtt-expressing MSNs than that observed in YAC18 (inset, NMDAR currents shown in *C* peak scaled to I_{AMPA} peak amplitudes, above respective genotypes). *E*, isolated NMDAR eEPSC slow component decay time constants are significantly longer in YAC128(53) than YAC18 MSNs. *F*, normalized current–voltage relationships demonstrate that Mg^{2+} sensitivity is equivalent across genotypes. $^*P < 0.05$, $^{**}P < 0.01$, $^{***}P < 0.001$.

effect of genotype ($P < 0.02$, $F_{3,94} = 3.71$); Bonferroni *post hoc* analysis demonstrated at a stimulus intensity of 150 μA, I_{AMPA} peaks were significantly smaller in YAC72 and YAC128(53) MSNs than those recorded in YAC18 MSNs (YAC72, 1059.8 ± 146.3 pA, $n = 19$, $P < 0.05$; YAC128(53), 768.4 ± 124.8 pA, $n = 7$, $P < 0.01$; YAC18, 1542.5 ± 246.8 pA, $n = 11$). A similar trend was observed at the 50 μA stimulation intensity, although differences were not significant (Fig. 4*A*), nor were there any significant differences in I_{AMPA} decay rates by ANOVA (Fig. 4*B*). The data suggest that AMPAR current peaks are similar across genotypes at lower stimulus intensities, but that high levels of stimulation reveal reduced AMPAR-mediated eEPSC amplitudes in mhtt-expressing mice. The lack of any alteration in AMPAR sEPSC amplitudes (Fig. 1), together with reduced P_r (Fig. 2), observed in YAC72 MSNs, suggests that smaller AMPAR eEPSCs found in these neurons are wholly attributable to presynaptic dysfunction, and not AMPAR alterations. On the other hand, the further reduction in AMPAR eEPSC amplitudes in YAC128(53) MSNs is probably attributable to a combination of reduced P_r (Fig. 2) and altered AMPAR number and/or subunit composition (Fig. 1).

To assess NMDAR-mediated current, cells were voltage-clamped at +60 mV to relieve voltage-dependent Mg^{2+} block of the NMDAR pore, and dual AMPAR/NMDAR eEPSCs were evoked (150 μA stimulation). In initial experiments, concomitant field recordings were utilized to assay drug delivery efficacy and current characterization. The majority of current recorded under these conditions is NMDAR-mediated; addition of the NMDAR antagonist D-AP5 had no discernable effect upon the predominantly AMPAR/population spike-mediated field potential or sEPSCs; however, the slow NMDAR-mediated component of dual currents was entirely abolished in < 5 min (not shown). Addition of the AMPAR antagonist CNQX effectively silenced AMPAR-mediated transmission, leaving pharmacologically isolated NMDAR currents (Fig. 4*C*, inset).

I_{NMDA} quantification is shown in Fig. 4*C*. Two-way ANOVA demonstrated no significant effect of genotype upon NMDAR-mediated current amplitude ($P > 0.05$). However, the magnitude of currents generated by a known intensity of afferent stimulation is affected by several factors other than postsynaptic receptor number. Aside from alterations in P_r, another major factor is the number of afferents activated, which is dependent upon variables such as electrode placement and slice viability. Therefore, measures of evoked current amplitude alone are not necessarily a good means to compare postsynaptic responsiveness. With this in mind, AMPAR-mediated eEPSCs (V_h −70 mV) were compared with pharmacologically isolated evoked NMDAR currents from the same cell (and stimulation) in order to calculate an NMDAR : AMPAR current ratio for each individual neurone. This provides a measure of NMDAR activity relative to that of AMPAR activity (and thus glutamatergic input), regardless of the number of presynaptic afferents recruited or P_r.

The calculated NMDAR- to AMPAR-mediated current ratio demonstrates an increased NMDAR contribution to synaptic transmission relative to AMPAR current in mhtt-expressing MSNs (Fig. 4*D*). One-way ANOVA demonstrated a significant effect of genotype ($P < 0.03$, $H = 9.01$); direct comparisons revealed that the NMDAR : AMPAR ratio was significantly greater in YAC72 (1.15 ± 0.13, $n = 19$, $P < 0.01$), YAC128(55) (1.19 ± 0.17, $n = 16$, $P < 0.05$), and YAC128(53) (1.22 ± 0.09, $n = 7$, $P < 0.001$) MSNs, than that observed in YAC18 (0.71 ± 0.07, $n = 11$). The results demonstrate an increase in the relative number of NMDARs at the postsynaptic locale in mhtt-expressing MSNs, with respect to AMPAR for any given degree of glutamate release. The lack of any difference in AMPAR sEPSC amplitudes (Fig. 1), together with the an elevated NMDAR : AMPAR current ratio (Fig. 4) suggests specifically increased NMDAR numbers in YAC72 and YAC128(55) MSNs, whereas reductions in AMPAR numbers/kinetics may also contribute to the altered ratio in YAC128(53) MSNs.

The kinetics of NMDAR currents are determined by receptor subunit composition (reviewed in Dingledine *et al.* 1999), notably NR2B/C/D-subunit containing receptors exhibit slower decay rates than those containing NR2A-subunits (Vicini *et al.* 1998). Therefore, we analysed the decay kinetics of I_{NMDA}, with a double exponential fit placed from peak to 2000 ms (Fig. 4*E*). One-way ANOVA demonstrated no significant ($P = 0.9$) difference in weighted decay constant (τ_W) between genotypes; however, there was a significant effect of both genotype, and genotype–τ interaction by two-way ANOVA of the 'fast' decay constant (τ_f) and 'slow' decay time constants (τ_s) which underlie τ_W (interaction, $P < 0.02$, $F_{3,52} = 3.9$). Bonferroni *post hoc* analysis demonstrated highly significant ($P < 0.001$) increases in τ_s for YAC128(53) MSNs relative to YAC18. Additionally, we noted that the percentage of peak fit by the fast and slow time constants ($\tau_s = 69 \pm 0.04, 69 \pm 0.02, 66 \pm 0.04, 58 \pm 0.08\%$ for YAC18, 72, 128(55) and 128(53), respectively) also showed a trend towards difference ($P = 0.08$ for greater percentage τ_f in YAC128(53)), an observation that accounts for the lack of significant change in τ_W. Together the data suggest that mhtt-expressing MSNs exhibit polyQ length-dependent alterations in kinetics that may reflect a shift in subunit composition; although, we have previously reported that NMDAR currents in WT and YAC72 MSNs are entirely insensitive to the NR1/2B-subunit-selective antagonist ifenprodil (Li *et al.* 2004), as are those in YAC128 MSNs (not shown). Alternatively, this slowing may be attributable to the

activation of a larger proportion of peri-/extra-synaptic receptors in mhtt-expressing MSNs (see Discussion).

The contribution of NMDARs to corticostriatal transmission at physiologically hyperpolarized membrane potentials is regulated by sensitivity to voltage-dependent Mg^{2+} block in the pore, notably, altered NMDAR sensitivity to Mg^{2+} in striatal MSNs, as has been demonstrated elsewhere in other (early symptomatic) transgenic mouse models of HD (Starling *et al.* 2005; Andre *et al.* 2006). In contrast, analysis of the NMDAR component of eEPSCs at varying V_h in YAC transgenic mice (normalized to maximum negative current) demonstrated no alteration in Mg^{2+} sensitivity across genotypes at this presymptomatic age (Fig. 4*F*).

Discussion

Previous studies documented altered NMDAR function and toxicity in striatal MSNs in HD mouse models (Levine *et al.* 1999; Cepeda *et al.* 2001; Hansson *et al.* 2001; Laforet *et al.* 2001; Zeron *et al.* 2002; Li *et al.* 2004; Starling *et al.* 2005; Shehadeh *et al.* 2006; Fan *et al.* 2007), while others reported alterations in synaptic transmission within the corticostriatal pathway in the R6/2 mouse model (Cepeda *et al.* 2003, 2007). Although many of these studies have focused on the role of such changes in striatal neuronal loss in HD, altered corticostriatal transmission may contribute to early deficits in cognition and mood, which are commonly observed prior to motor onset of HD (Lawrence *et al.* 2000; Berrios *et al.* 2002; Paulsen *et al.* 2006*a*). Here, we report electrophysiological disturbances at the corticostriatal synapse in YAC HD mouse models, which occur prior to motor deficits and show increasing severity with increasing mhtt expression level and polyQ length. YAC72 and YAC128(55) synapses exhibited specifically increased NMDAR current relative to AMPAR current, in addition to reduced P_r, when compared to YAC18. The most severe model, YAC128(53), exhibited similarly altered NMDAR current and P_r, in addition to AMPAR alterations. Separately, we also found significant polyQ length-dependent depression of synaptic transmission. These findings demonstrate multiple premanifest perturbations to corticostriatal function in HD mice, and further our understanding of the early effects of the HD mutation.

Mutant huntingtin and altered AMPA receptor-mediated transmission

In YAC128(53) MSNs, evoked AMPAR peaks were reduced. Although the observed decrease in P_r probably contributed to smaller evoked amplitudes, the concomitant shift towards smaller amplitude sEPSCs demonstrates that postsynaptic AMPAR responsiveness is lower in YAC128(53) MSNs. Although bias in event collection (i.e. inclusion of more small events) might contribute to increased frequency of small amplitude sEPSCs, a reduced frequency of medium-sized events was also observed. Additionally, AMPAR decay kinetics were significantly faster. Together, three lines of evidence suggest AMPAR number, subunit composition, and/or trafficking are perturbed at an early age by high expression of mhtt with a large polyQ expansion.

While AMPAR sEPSC frequencies are reduced in MSNs of symptomatic R6/2 HD mice, amplitudes and decay kinetics are unaltered (Cepeda *et al.* 2003), suggesting the presymptomatic changes observed in our study are distinct to full-length mhtt. On the other hand, R6/2 cortical neurons show decreased AMPAR current amplitudes and altered cyclothiazide sensitivity, indicating an increased proportion of 'flop' splice variant AMPAR subunits (Andre *et al.* 2006). Interestingly, increased flop expression and accelerated EPSC decay rates occur developmentally (Koike-Tani *et al.* 2005) and, in striatal cells, flop-containing AMPARs are associated with faster EPSC kinetics (Vorobjev *et al.* 2000). Furthermore, increased striatal flop-variant AMPAR subunit mRNA expression occurs following cortical deafferentation (Wullner *et al.* 1994). Thus, faster AMPAR decay kinetics observed in YAC128(53) mice might reflect increased flop-containing receptors, a process potentially driven by reduced corticostriatal signalling.

Synaptic AMPAR numbers are subject to dynamic regulation through activity-dependent Ca^{2+} signalling (Gerdeman *et al.* 2003; Nicoll, 2003; Sutton *et al.* 2006; Thiagarajan *et al.* 2007) and are therefore likely to change in the face of altered transmission, including NMDAR and/or dopamine receptor signalling (Price *et al.* 1999; Snyder *et al.* 2000, 2003; reviewed in Surmeier *et al.* 2007). The HD mutation directly disrupts the function of several htt-interacting proteins, which could potentially lead to altered receptor function (reviewed in Li & Li, 2004; and Milnerwood & Raymond, 2006). For example, HIP1 is a regulator of AMPAR trafficking (Kalchman *et al.* 1997; Wanker *et al.* 1997; Metzler *et al.* 2001, 2003; Waelter *et al.* 2001; Rao *et al.* 2003) and HIP14 (Singaraja *et al.* 2002) regulates membrane association of (amongst other targets) PSD-95 (Ducker *et al.* 2004; Huang *et al.* 2004).

Presynaptic dysfunction

We observed significantly increased PPF, indicating reduced P_r at the mhtt-expressing corticostriatal synapse. Smaller AMPAR eEPSC amplitudes may partially be a result of reduced P_r, but it is also possible that smaller responses generally exhibit a differing P_r; however, there was no correlation between initial eEPSC amplitude and PPF (not shown). Furthermore, the PPF ratios measured for small YAC18 currents were consistently lower than those of YAC128 currents of equal magnitude.

Presynaptic dysfunction has also been reported in symptomatic R6/2 striatum (Klapstein *et al.* 2001; Cepeda *et al.* 2003) and asymptomatic knock-in mouse hippocampus (Usdin *et al.* 1999). In contrast to our findings, and those of Cepeda *et al.*, two investigations of PPF showed it was reduced, although it was also noted that greater stimulus intensities were required to generate EPSPs (Klapstein *et al.* 2001) and that transmitter release could not be sustained over time (Usdin *et al.* 1999) in these studies (also see penultimate paragraph). Reduced P_r may be specific to the striatum, as no differences in PPF are observed in symptomatic R6/2 hippocampus (Murphy *et al.* 2000), or in the hippocampus (Milnerwood *et al.* 2006*a*) and cortex (Dallerac *et al.* 2006) of R6/1 mice at pre- or postsymptomatic stages.

Despite the increased PPF we found, there were no significant changes in mean interevent intervals or mean cell event frequencies. It is possible that the source of disparity is differential presynaptic calcium signalling between evoked and spontaneous activity and that the dysfunction is therefore specific to action potential-dependent release and not mEPSCs, as the two have been proposed to be mechanistically distinct (Sara *et al.* 2005); however, this proposition has recently been challenged (Groemer & Klingauf, 2007). It is perhaps more likely that the presynaptic defect is subtle, exists for both miniature and AP-dependent release, yet is only readily observed in the large number of synaptic events that underlie evoked EPSCs. That said, both YAC128 mouse lines had significantly greater variance in mean IEIs than found for YAC18 or YAC72, and ∼25% of MSNs in YAC18 and YAC72 slices had mean sEPSC frequencies greater than the maximum observed in either YAC128 model. Interestingly, indirect pathway MSNs, which degenerate first in HD (Glass *et al.* 2000), exhibit mEPSC frequencies approximately double that of direct pathway MSNs (Kreitzer & Malenka, 2007), raising the possibility that we may have observed reduced mean frequency in a subset (indirect pathway) of MSNs in our mixed sample.

Alteration of htt protein interactions by polyQ expansion may directly underlie presynaptic dysfunction (reviewed in Milnerwood, 2006). For example, clathrin-mediated vesicular endocytosis (Owen, 2004) and glutamate release are regulated by HIP1 (Metzler *et al.* 2001; Li *et al.* 2003), and the vesicular release proteins SNAP-25 and synaptotagmin are palmitoylated by HIP14 (Huang *et al.* 2004); disruption of these interactions by mhtt is evidence for 'loss of function' effects. 'Gain of function' effects may also be important in the HD vesicle cycle, e.g. htt binding to PACSIN1 (a regulator of vesicle recovery) is increased proportionally to polyQ repeat length, and PACSIN1 is abnormally distributed away from synaptic compartments in HD tissue (Modregger *et al.* 2002; DiProspero *et al.* 2004).

Increased NMDAR signalling

NMDAR : AMPAR current ratios were increased in all expanded repeat genotypes relative to YAC18, suggesting mhtt increases postsynaptic NMDAR current. The presynaptic dysfunction observed in mhtt-expressing MSNs may explain why NMDAR currents were not larger *per se*, and why eliminating presynaptic differences by analysing the NMDAR : AMPAR current ratio revealed increased postsynaptic NMDAR responsiveness. Although smaller AMPAR numbers would also affect this ratio, the similar amplitude of AMPAR sEPSCs in WT, YAC72 and YAC128(55) MSNs indicated that the increased NMDAR : AMPAR ratio in the latter two mouse lines reflects increased NMDAR current. In contrast, reduced AMPAR currents in YAC128(53) MSNs are likely to further contribute to increased NMDAR : AMPAR ratio.

MSNs *in vivo* display characteristic upstate and downstate shifts, which regulate action potential generation (Wilson & Kawaguchi, 1996). Highly integrated cortical input is required for upstate shifting, and modelling studies suggest NMDAR : AMPAR current ratios critically regulate transitions; increased NMDAR components result in the failure of MSNs to entrain to afferent input and generate action potentials (Wolf *et al.* 2005). Thus, a major effect of increased NMDAR current described here may be reduced striatal output, regardless of excitatory drive.

We observed significant slowing of the NMDAR EPSC decay constant slow component in YAC128(53) MSNs. One possible explanation would be altered NMDAR subunit composition (reviewed in Dingledine *et al.* 1999), i.e. a greater contribution of NR2B/C/D-subunit-containing receptors (Vicini *et al.* 1998). A lack of ifenprodil sensitivity in WT, YAC72 (Li *et al.* 2004) and YAC128 (not shown) NMDAR currents suggests that corticostriatal synapses contain triheteromeric NR1/NR2A/NR2B receptors (*ibid.*). Although this rules out an increased contribution of NR2B subunits within single NMDARs (containing two NR1 and two NR2 subunits) in YAC128(53) MSNs, these triheteromeric receptors may be proportionally increased with respect to NR1/NR2A. Alternatively, ongoing studies in our laboratory suggest that extrasynaptic NMDAR currents, shown by others to promote cell death (Hardingham & Bading, 2002), are also greatly enhanced (authors' unpublished observations and see Milnerwood *et al.* 2006*b*; Fan *et al.* 2007). Thus, slowing of NMDAR EPSC decay in YAC128 MSNs might reflect activation of NMDARs located some distance from the release site (Massey *et al.* 2004; Scimemi *et al.* 2004). Further experiments are required to determine the mechanism underlying slowing of NMDAR EPSC decay in YAC128(53) MSNs.

The HD corticostriatal synapse

Striatal long-term depression (LTD), induced by post-synaptic Ca^{2+}-triggered endocannabinoid release, is expressed presynaptically as reduced P_r (Gerdeman *et al.* 2002; Ronesi *et al.* 2004; Kreitzer & Malenka, 2005, 2007; Ronesi & Lovinger, 2005). Interestingly, in addition to elevated NMDAR currents, we observed decreased presynaptic release in mhtt-expressing YAC MSNs. In separate experiments, upon prolonged stimulation, we observed large reductions of eEPSC amplitude over time in mhtt-expressing YAC MSNs (Fig. 3). Separately, we also found that YAC72 currents, unlike those of YAC18 mice, were unable to sustain the 20% frequency-dependent increase produced throughout 30 shocks delivered at 10 Hz (not shown). Many factors could contribute to this activity-dependent depression, from dialysis of cellular contents and/or depletion of critical intracellular factors, to altered dopaminergic and/or endocannabinoid signalling, or alterations in sustained presynaptic release over time; further investigation will be required to determine the underlying mechanism. Our findings suggest that the HD corticostriatal synapse exhibits an increased propensity towards depression. These data are consistent with reports of impaired hippocampal (Usdin *et al.* 1999; Murphy *et al.* 2000; Milnerwood *et al.* 2006*a*; Lynch *et al.* 2007) and cortical (Dallerac *et al.* 2006) LTP, and reports of increased hippocampal (Milnerwood *et al.* 2006*a*) and cortical (Cummings *et al.* 2006) LTD at presymptomatic stages in other HD mouse models. Taken together, these reports suggest synaptic transmission in HD is intrinsically unstable.

Our results suggest attempts to increase AMPAR signalling (Lynch, 2006; Lynch *et al.* 2007), or otherwise reverse the postulated corticostriatal disconnect (Cepeda *et al.* 2007) may prove beneficial as therapy in early HD. One of the perturbations reported here furthest from phenotypic onset (and seen in MSNs cultured from birth) – augmented NMDAR signalling – may be a mechanism by which other disturbances develop. Unfortunately, as they are critical to many physiological processes, pharmacological inhibition of NMDARs has had limited benefits and serious side-effects (Chen & Lipton, 2006). However, ongoing investigations concerning mhtt-induced alterations in subcellular NMDAR trafficking (Milnerwood *et al.* 2006*b*; Fan *et al.* 2007), in what appears to be a tightly regulated system (reviewed in Prybylowski *et al.* 2005; Lau & Zukin, 2007), offer hope for highly specific drug targets.

References

Andre VM, Cepeda C, Venegas A, Gomez Y & Levine MS (2006). Altered cortical glutamate receptor function in the R6/2 model of Huntington's disease. *J Neurophysiol* **95**, 2108–2119.

Aronin N, Chase K, Young C, Sapp E, Schwarz C, Matta N, Kornreich R, Landwehrmeyer B, Bird E, Beal MF *et al*. (1995). CAG expansion affects the expression of mutant Huntingtin in the Huntington's disease brain. *Neuron* **15**, 1193–1201.

Beal MF (1992). Role of excitotoxicity in human neurological disease. *Curr Opin Neurobiol* **2**, 657–662.

Berrios GE, Wagle AC, Marková IS, Wagle SA, Rosser A & Hodges JR (2002). Psychiatric symptoms in neurologically asymptomatic Huntington's disease gene carriers: a comparison with gene negative at risk subjects. *Acta Psychiatr Scand* **105**, 224–230.

Bliss TVP & Collingridge GL (1993). A synaptic model of memory: long-term potentiation in the hippocampus. *Nature* **361**, 31–39.

Cepeda C, Ariano MA, Calvert CR, Flores-Hernandez J, Chandler SH, Leavitt BR, Hayden MR & Levine MS (2001). NMDA receptor function in mouse models of Huntington disease. *J Neurosci Res* **66**, 525–539.

Cepeda C, Hurst RS, Calvert CR, Hernandez-Echeagaray E, Nguyen OK, Jocoy E, Christian LJ, Ariano MA & Levine MS (2003). Transient and progressive electrophysiological alterations in the corticostriatal pathway in a mouse model of Huntington's disease. *J Neurosci* **23**, 961–969.

Cepeda C, Wu N, Andre VM, Cummings DM & Levine MS (2007). The corticostriatal pathway in Huntington's disease. *Prog Neurobiol* **81**, 253–271.

Chen HS & Lipton SA (2006). The chemical biology of clinically tolerated NMDA receptor antagonists. *J Neurochem* **97**, 1611–1626.

Choi DW (1992). Excitotoxic cell death. *J Neurobiol* **23**, 1261–1276.

Cummings DM, Milnerwood AJ, Dallerac GM, Vatsavayai SC, Hirst MC & Murphy KP (2007). Abnormal cortical synaptic plasticity in a mouse model of Huntington's disease. *Brain Res Bull* **72**, 103–107.

Cummings DM, Milnerwood AJ, Dallerac GM, Waights V, Brown JY, Vatsavayai SC, Hirst MC & Murphy KP (2006). Aberrant cortical synaptic plasticity and dopaminergic dysfunction in a mouse model of Huntington's disease. *Human Mol Genet* **15**, 2856–2868.

Dallerac GM, Vatsavayai SC, Cummings DM, Milnerwood AJ, Hirst MC & Murphy KPSJ (2006). Impaired long-term potentiation (LTP) at prefrontal cortical synapses and dopaminergic rescue in Huntington's disease mice. *Abstract Viewer/Itinerary Planner, Society for Neuroscience, Washington, DC*. Abstract No. 472.6

DiFiglia M, Sapp E, Chase K, Schwarz C, Meloni A, Young C, Martin E, Vonsattel JP, Carraway R, Reeves SA *et al*. (1995). Huntingtin is a cytoplasmic protein associated with vesicles in human and rat brain neurons. *Neuron* **14**, 1075–1081.

Dingledine R, Borges K, Bowie D & Traynelis SF (1999). The glutamate receptor ion channels. *Pharmacol Rev* **51**, 7–61.

DiProspero NA, Chen EY, Charles V, Plomann M, Kordower JH & Tagle DA (2004). Early changes in Huntington's disease patient brains involve alterations in cytoskeletal and synaptic elements. *J Neurocytol* **33**, 517–533.

Ducker CE, Stettler EM, French KJ, Upson JJ & Smith CD (2004). Huntingtin interacting protein 14 is an oncogenic human protein: palmitoyl acyltransferase. *Oncogene* **23**, 9230–9237.

Duff K, Paulsen JS, Beglinger LJ, Langbehn DR, Stout JC & the Predict-HD Investigators of the Huntington Study Group (2007). Psychiatric symptoms in Huntington's disease before diagnosis: The Predict-HD Study. *Biol psychiatry* (in press); DOI: 10.1016/j.biopsych.2006.11.034.

Duyao M, Ambrose C, Myers R, Novelletto A, Persichetti F, Frontali M, Folstein S, Ross C, Franz M, Abbott M *et al*. (1993). Trinucleotide repeat length instability and age of onset in Huntington's disease. *Nat Genet* **4**, 387–392.

Fan MM, Fernandes HB, Zhang LY, Hayden MR & Raymond LA (2007). Altered NMDA receptor trafficking in a yeast artificial chromosome transgenic mouse model of Huntington's disease. *J Neurosci* **27**, 3768–3779.

Fan MM & Raymond LA (2007). *N*-methyl-D-aspartate (NMDA) receptor function and excitotoxicity in Huntington's disease. *Prog Neurobiol* **81**, 272–293.

Gerdeman GL, Partridge JG, Lupica CR & Lovinger DM (2003). It could be habit forming: drugs of abuse and striatal synaptic plasticity. *Trends Neurosci* **26**, 184–192.

Gerdeman GL, Ronesi J & Lovinger DM (2002). Postsynaptic endocannabinoid release is critical to long-term depression in the striatum. *Nat Neurosci* **5**, 446–451.

Glass M, Dragunow M & Faull RL (2000). The pattern of neurodegeneration in Huntington's disease: a comparative study of cannabinoid, dopamine, adenosine and $GABA_A$ receptor alterations in the human basal ganglia in Huntington's disease. *Neuroscience* **97**, 505–519.

Graham RK, Slow EJ, Deng Y, Bissada N, Lu G, Pearson J, Shehadeh J, Leavitt BR, Raymond LA & Hayden MR (2006). Levels of mutant huntingtin influence the phenotypic severity of Huntington disease in YAC128 mouse models. *Neurobiol Dis* **21**, 444–455.

Groemer TW & Klingauf J (2007). Synaptic vesicles recycling spontaneously and during activity belong to the same vesicle pool. *Nat Neurosci* **10**, 145–147.

Gunawardena S, Her LS, Brusch RG, Laymon RA, Niesman IR, Gordesky-Gold B, Sintasath L, Bonini NM & Goldstein LS (2003). Disruption of axonal transport by loss of huntingtin or expression of pathogenic polyQ proteins in *Drosophila*. *Neuron* **40**, 25–40.

Hansson O, Guatteo E, Mercuri NB, Bernardi G, Li XJ, Castilho RF & Brundin P (2001). Resistance to NMDA toxicity correlates with appearance of nuclear inclusions, behavioural deficits and changes in calcium homeostasis in mice transgenic for exon 1 of the huntington gene. *Eur J Neurosci* **14**, 1492–1504.

Hardingham GE (2006). Pro-survival signalling from the NMDA receptor. *Biochem Soc Trans* **34**, 936–938.

Hardingham GE & Bading H (2002). Coupling of extrasynaptic NMDA receptors to a CREB shut-off pathway is developmentally regulated. *Biochim Biophys Acta* **1600**, 148–153.

HDCRG (1993). A novel gene containing a trinucleotide repeat that is expanded and unstable on Huntington's disease chromosomes. The Huntington's Disease Collaborative Research Group. *Cell* **72**, 971–983.

Hodgson JG, Agopyan N, Gutekunst CA, Leavitt BR, LePiane F, Singaraja R, Smith DJ, Bissada N, McCutcheon K, Nasir J, Jamot L, Li XJ, Stevens ME, Rosemond E, Roder JC, Phillips AG, Rubin EM, Hersch SM & Hayden MR (1999). A YAC mouse model for Huntington's disease with full-length mutant huntingtin, cytoplasmic toxicity, and selective striatal neurodegeneration. *Neuron* **23**, 181–192.

Huang K, Yanai A, Kang R, Arstikaitis P, Singaraja RR, Metzler M, Mullard A, Haigh B, Gauthier-Campbell C, Gutekunst CA, Hayden MR & El-Husseini A (2004). Huntingtin-interacting protein HIP14 is a palmitoyl transferase involved in palmitoylation and trafficking of multiple neuronal proteins. *Neuron* **44**, 977–986.

Kalchman MA, Koide HB, McCutcheon K, Graham RK, Nichol K, Nishiyama K, Kazemi-Esfarjani P, Lynn FC, Wellington C, Metzler M, Goldberg YP, Kanazawa I, Gietz RD & Hayden MR (1997). *HIP1*, a human homologue of *S. cerevisiae Sla2p*, interacts with membrane-associated huntingtin in the brain. *Nat Genet* **16**, 44–53.

Klapstein GJ, Fisher RS, Zanjani H, Cepeda C, Jokel ES, Chesselet MF & Levine MS (2001). Electrophysiological and morphological changes in striatal spiny neurons in R6/2 Huntington's disease transgenic mice. *J Neurophysiol* **86**, 2667–2677.

Koike-Tani M, Saitoh N & Takahashi T (2005). Mechanisms underlying developmental speeding in AMPA-EPSC decay time at the calyx of Held. *J Neurosci* **25**, 199–207.

Kreitzer AC & Malenka RC (2005). Dopamine modulation of state-dependent endocannabinoid release and long-term depression in the striatum. *J Neurosci* **25**, 10537–10545.

Kreitzer AC & Malenka RC (2007). Endocannabinoid-mediated rescue of striatal LTD and motor deficits in Parkinson's disease models. *Nature* **445**, 643–647.

Laforet GA, Sapp E, Chase K, McIntyre C, Boyce FM, Campbell M, Cadigan BA, Warzecki L, Tagle DA, Reddy PH, Cepeda C, Calvert CR, Jokel ES, Klapstein GJ, Ariano MA, Levine MS, DiFiglia M & Aronin N (2001). Changes in cortical and striatal neurons predict behavioral and electrophysiological abnormalities in a transgenic murine model of Huntington's disease. *J Neurosci* **21**, 9112–9123.

Landwehrmeyer GB, McNeil SM, St Dure L, Ge P, Aizawa H, Huang Q, Ambrose CM, Duyao MP, Bird ED, Bonilla E, de Young M, Avila-Gonzales AJ, Wexler NS, DiFiglia M, Gusella JF, MacDonald ME, Penney JB, Young AB & Vonsattel J-P (1995). Huntington's disease gene: Regional and cellular expression in brain of normal and affected individuals. *Ann Neurol* **37**, 218–230.

Lau CG & Zukin RS (2007). NMDA receptor trafficking in synaptic plasticity and neuropsychiatric disorders. *Nat Rev* **8**, 413–426.

Lawrence AD, Watkins LH, Sahakian BJ, Hodges JR & Robbins TW (2000). Visual object and visuospatial cognition in Huntington's disease: Implications for information processing in corticostriatal circuits. *Brain* **123**, 1349–1364.

Levine MS, Klapstein GJ, Koppel A, Gruen E, Cepeda C, Vargas ME, Jokel ES, Carpenter EM, Zanjani H, Hurst RS, Efstratiadis A, Zeitlin S & Chesselet MF (1999). Enhanced sensitivity to *N*-methyl-D-aspartate receptor activation in transgenic and knockin mouse models of Huntington's disease. *J Neurosci Res* **58**, 515–532.

Li SH & Li XJ (2004). Huntingtin–protein interactions and the pathogenesis of Huntington's disease. *Trends Genet* **20**, 146–154.

Li H, Li SH, Yu ZX, Shelbourne P & Li XJ (2001). Huntingtin aggregate-associated axonal degeneration is an early pathological event in Huntington's disease mice. *J Neurosci* **21**, 8473–8481.

Li L, Murphy TH, Hayden MR & Raymond LA (2004). Enhanced striatal NR2B-containing *N*-methyl-D-aspartate receptor-mediated synaptic currents in a mouse model of Huntington disease. *J Neurophysiol* **92**, 2738–2746.

Li H, Wyman T, Yu ZX, Li SH & Li XJ (2003). Abnormal association of mutant huntingtin with synaptic vesicles inhibits glutamate release. *Hum Mol Genet* **12**, 2021–2030.

Lisman J (2003). Long-term potentiation: Outstanding questions and attempted synthesis. *Philos Trans R Soc Lond B Biol Sci* **358**, 829–842.

Lynch G (2006). Glutamate-based therapeutic approaches: ampakines. *Curr Opin Pharmacol* **6**, 82–88.

Lynch G, Kramar EA, Rex CS, Jia Y, Chappas D, Gall CM & Simmons DA (2007). Brain-derived neurotrophic factor restores synaptic plasticity in a knock-in mouse model of Huntington's disease. *J Neurosci* **27**, 4424–4434.

Massey PV, Johnson BE, Moult PR, Auberson YP, Brown MW, Molnar E, Collingridge GL & Bashir ZI (2004). Differential roles of NR2A and NR2B-containing NMDA receptors in cortical long-term potentiation and long-term depression. *J Neurosci* **24**, 7821–7828.

Mazarakis NK, Cybulska-Klosowicz A, Grote H, Pang T, Van Dellen A, Kossut M, Blakemore C & Hannan AJ (2005). Deficits in experience-dependent cortical plasticity and sensory-discrimination learning in presymptomatic Huntington's disease mice. *J Neurosci* **25**, 3059–3066.

Metzler M, Legendre-Guillemin V, Gan L, Chopra V, Kwok A, McPherson PS & Hayden MR (2001). HIP1 functions in clathrin-mediated endocytosis through binding to clathrin and adaptor protein 2. *J Biol Chem* **276**, 39271–39276.

Metzler M, Li B, Gan L, Georgiou J, Gutekunst CA, Wang Y, Torre E, Devon RS, Oh R, Legendre-Guillemin V, Rich M, Alvarez C, Gertsenstein M, McPherson PS, Nagy A, Wang YT, Roder JC, Raymond LA & Hayden MR (2003). Disruption of the endocytic protein HIP1 results in neurological deficits and decreased AMPA receptor trafficking. *EMBO J* **22**, 3254–3266.

Milnerwood AJ, Cummings DM, Dallerac GM, Brown JY, Vatsavayai SC, Hirst MC, Rezaie P & Murphy KP (2006*a*). Early development of aberrant synaptic plasticity in a mouse model of Huntington's disease. *Hum Mol Genet* **15**, 1690–1703.

Milnerwood AJ, Hayden MR, Murphy T & Raymond LA (2006*b*). Corticostriatal dysfunction in mouse models of Huntington's disease. *Abstract Viewer/Itinerary Planner, Society for Neuroscience*, *Washington*, *DC*; Program No. 472.417.

Milnerwood AJ & Raymond LA (2006). Synaptic abnormalities associated with Huntington's disease. In *Molecular Mechanisms of Synaptogenesis*, ed.El-Husseini A, Dityatev A, pp. 457–469. Springer, New York.

Modregger J, DiProspero NA, Charles V, Tagle DA & Plomann M (2002). PACSIN 1 interacts with huntingtin and is absent from synaptic varicosities in presymptomatic Huntington's disease brains. *Hum Mol Genet* **11**, 2547–2558.

Murphy KPSJ, Carter RJ, Lione LA, Mangiarini L, Mahal A, Bates GP, Dunnett SB & Morton AJ (2000). Abnormal synaptic plasticity and impaired spatial cognition in mice transgenic for exon 1 of the human Huntington's disease mutation. *J Neurosci* **20**, 5115–5123.

Nicoll RA (2003). Expression mechanisms underlying long-term potentiation: a postsynaptic view. *Philos Trans R Soc Lond B Biol Sci* **358**, 721–726.

Owen DJ (2004). Linking endocytic cargo to clathrin: structural and functional insights into coated vesicle formation. *Biochem Soc Trans* **32**, 1–14.

Paulsen JS, Hayden M, Stout JC, Langbehn DR, Aylward E, Ross CA, Guttman M, Nance M, Kieburtz K, Oakes D, Shoulson I, Kayson E, Johnson S & Penziner E (2006*a*). Preparing for preventive clinical trials: the Predict-HD study. *Arch Neurol* **63**, 883–890.

Paulsen JS, Magnotta VA, Mikos AE, Paulson HL, Penziner E, Andreasen NC & Nopoulos PC (2006*b*). Brain structure in preclinical Huntington's disease. *Biol Psychiatry* **59**, 57–63.

Pláteník J, Kuramoto N & Yoneda Y (2000). Molecular mechanisms associated with long-term consolidation of the NMDA signals. *Life Sci* **67**, 335–364.

Price CJ, Kim P & Raymond LA (1999). D1 dopamine receptor-induced cyclic AMP-dependent protein kinase phosphorylation and potentiation of striatal glutamate receptors. *J Neurochem* **73**, 2441–2446.

Prybylowski K, Chang K, Sans N, Kan L, Vicini S & Wenthold RJ (2005). The synaptic localization of NR2B-containing NMDA receptors is controlled by interactions with PDZ proteins and AP-2. *Neuron* **47**, 845–857.

Rao DS, Bradley SV, Kumar PD, Hyun TS, Saint-Dic D, Oravecz-Wilson K, Kleer CG & Ross TS (2003). Altered receptor trafficking in Huntingtin Interacting Protein 1-transformed cells. *Cancer Cell* **3**, 471–482.

Ronesi J, Gerdeman GL & Lovinger DM (2004). Disruption of endocannabinoid release and striatal long-term depression by postsynaptic blockade of endocannabinoid membrane transport. *J Neurosci* **24**, 1673–1679.

Ronesi J & Lovinger DM (2005). Induction of striatal long-term synaptic depression by moderate frequency activation of cortical afferents in rat. *J Physiol* **562**, 245–256.

Sara Y, Virmani T, Deak F, Liu X & Kavalali ET (2005). An isolated pool of vesicles recycles at rest and drives spontaneous neurotransmission. *Neuron* **45**, 563–573.

Scimemi A, Fine A, Kullmann DM & Rusakov DA (2004). NR2B-containing receptors mediate cross talk among hippocampal synapses. *J Neurosci* **24**, 4767–4777.

Shehadeh J, Fernandes HB, Zeron Mullins MM, Graham RK, Leavitt BR, Hayden MR & Raymond LA (2006). Striatal neuronal apoptosis is preferentially enhanced by NMDA receptor activation in YAC transgenic mouse model of Huntington disease. *Neurobiol Dis* **21**, 392–403.

Singaraja RR, Hadano S, Metzler M, Givan S, Wellington CL, Warby S, Yanai A, Gutekunst CA, Leavitt BR, Yi H, Fichter K, Gan L, McCutcheon K, Chopra V, Michel J, Hersch SM, Ikeda JE & Hayden MR (2002). HIP14, a novel ankyrin domain-containing protein, links huntingtin to intracellular trafficking and endocytosis. *Hum Mol Genet* **11**, 2815–2828.

Slow EJ, van Raamsdonk J, Rogers D, Coleman SH, Graham RK, Deng Y, Oh R, Bissada N, Hossain SM, Yang YZ, Li XJ, Simpson EM, Gutekunst CA, Leavitt BR & Hayden MR (2003). Selective striatal neuronal loss in a YAC128 mouse model of Huntington disease. *Hum Mol Genet* **12**, 1555–1567.

Snyder GL, Allen PB, Fienberg AA, Valle CG, Huganir RL, Nairn AC & Greengard P (2000). Regulation of phosphorylation of the GluR1 AMPA receptor in the neostriatum by dopamine and psychostimulants *in vivo*. *J Neurosci* **20**, 4480–4488.

Snyder GL, Galdi S, Fienberg AA, Allen P, Nairn AC & Greengard P (2003). Regulation of AMPA receptor dephosphorylation by glutamate receptor agonists. *Neuropharmacology* **45**, 703–713.

Solomon AC, Stout JC, Johnson SA, Langbehn DR, Aylward EH, Brandt J, Ross CA, Beglinger L, Hayden MR, Kieburtz K, Kayson E, Julian-Baros E, Duff K, Guttman M, Nance M, Oakes D, Shoulson I, Penziner E & Paulsen JS (2007). Verbal episodic memory declines prior to diagnosis in Huntington's disease. *Neuropsychologia* **45**, 1767–1776.

Starling AJ, Andre VM, Cepeda C, de Lima M, Chandler SH & Levine MS (2005). Alterations in *N*-methyl-D-aspartate receptor sensitivity and magnesium blockade occur early in development in the R6/2 mouse model of Huntington's disease. *J Neurosci Res* **82**, 377–386.

Stocca G & Vicini S (1998). Increased contribution of NR2A subunit to synaptic NMDA receptors in developing rat cortical neurons. *J Physiol* **507**, 13–24.

Sudhof TC (2004). The synaptic vesicle cycle. *Annu Rev Neurosci* **27**, 509–547.

Surmeier DJ, Ding J, Day M, Wang Z & Shen W (2007). D1 and D2 dopamine-receptor modulation of striatal glutamatergic signaling in striatal medium spiny neurons. *Trends Neurosci* **30**, 228–235.

Sutton MA, Ito HT, Cressy P, Kempf C, Woo JC & Schuman EM (2006). Miniature neurotransmission stabilizes synaptic function via tonic suppression of local dendritic protein synthesis. *Cell* **125**, 785–799.

Szebenyi G, Morfini GA, Babcock A, Gould M, Selkoe K, Stenoien DL, Young M, Faber PW, MacDonald ME, McPhaul MJ & Brady ST (2003). Neuropathogenic forms of huntingtin and androgen receptor inhibit fast axonal transport. *Neuron* **40**, 41–52.

Thiagarajan TC, Lindskog M, Malgaroli A & Tsien RW (2007). LTP and adaptation to inactivity: overlapping mechanisms and implications for metaplasticity. *Neuropharmacology* **52**, 156–175.

Thomson AM (2000). Facilitation, augmentation and potentiation at central synapses. *Trends Neurosci* **23**, 305–312.

Trushina E, Dyer RB, Badger JD 2nd, Ure D, Eide L, Tran DD, Vrieze BT, Legendre-Guillemin V, McPherson PS, Mandavilli BS, Van Houten B, Zeitlin S, McNiven M, Aebersold R, Hayden M, Parisi JE, Seeberg E, Dragatsis I, Doyle K, Bender A, Chacko C & McMurray CT (2004). Mutant huntingtin impairs axonal trafficking in mammalian neurons in vivo and in vitro. *Mol Cell Biol* **24**, 8195–8209.

Usdin MT, Shelbourne PF, Myers RM & Madison DV (1999). Impaired synaptic plasticity in mice carrying the Huntington's disease mutation. *Human Mol Genet* **8**, 839–846.

Van Raamsdonk JM, Pearson J, Slow EJ, Hossain SM, Leavitt BR & Hayden MR (2005). Cognitive dysfunction precedes neuropathology and motor abnormalities in the YAC128 mouse model of Huntington's disease. *J Neurosci* **25**, 4169–4180.

Vicini S, Wang JF, Li JH, Zhu WJ, Wang YH, Luo JH, Wolfe BB & Grayson DR (1998). Functional and pharmacological differences between recombinant *N*-methyl-D-aspartate receptors. *J Neurophysiol* **79**, 555–566.

Vonsattel JP, Myers RH, Stevens TJ, Ferrante RJ, Bird ED & Richardson EP Jr (1985). Neuropathological classification of Huntington's disease. *J Neuropathol Exp Neurol* **44**, 559–577.

Vorobjev VS, Sharonova IN, Haas HL & Sergeeva OA (2000). Differential modulation of AMPA receptors by cyclothiazide in two types of striatal neurons. *Eur J Neurosci* **12**, 2871–2880.

Waelter S, Scherzinger E, Hasenbank R, Nordhoff E, Lurz R, Goehler H, Gauss C, Sathasivam K, Bates GP, Lehrach H & Wanker EE (2001). The huntingtin interacting protein HIP1 is a clathrin and α-adaptin-binding protein involved in receptor-mediated endocytosis. *Human Mol Genet* **10**, 1807–1817.

Wanker EE, Rovira C, Scherzinger E, Hasenbank R, Walter S, Tait D, Colicelli J & Lehrach H (1997). HIP-I: a huntingtin interacting protein isolated by the yeast two-hybrid system. *Hum Mol Genet* **6**, 487–495.

Wilson CJ & Kawaguchi Y (1996). The origins of two-state spontaneous membrane potential fluctuations of neostriatal spiny neurons. *J Neurosci* **16**, 2397–2410.

Wolf JA, Moyer JT, Lazarewicz MT, Contreras D, Benoit-Marand M, O'Donnell P & Finkel LH (2005). NMDA/AMPA ratio impacts state transitions and entrainment to oscillations in a computational model of the nucleus accumbens medium spiny projection neuron. *J Neurosci* **25**, 9080–9095.

Wu N, Cepeda CT, Zhuang X & Levine MS (2007). Altered corticostriatal neurotransmission and modulation in dopamine transporter knock-down mice. *J Neurophysiol* **98**, 423–432.

Wu XS, Xue L, Mohan R, Paradiso K, Gillis KD & Wu LG (2007). The origin of quantal size variation: vesicular glutamate concentration plays a significant role. *J Neurosci* **27**, 3046–3056.

Wullner U, Standaert DG, Testa CM, Landwehrmeyer GB, Catania MV, Penney JB Jr & Young AB (1994). Glutamate receptor expression in rat striatum: effect of deafferentation. *Brain Res* **647**, 209–219.

Yohrling GJ 4th & Cha JH (2002). Neurochemistry of Huntington's disease. In *Huntington's Disease*, 3rd edn, ed.Bates GP, Harper PS & Jones L, pp. 276–308. Oxford University Press, Oxford.

Zeron MM, Chen N, Moshaver A, Lee AT, Wellington CL, Hayden MR & Raymond LA (2001). Mutant huntingtin enhances excitotoxic cell death. *Mol Cell Neurosci* **17**, 41–53.

Zeron MM, Fernandes HB, Krebs C, Shehadeh J, Wellington CL, Leavitt BR, Baimbridge KG, Hayden MR & Raymond LA (2004). Potentiation of NMDA receptor-mediated excitotoxicity linked with intrinsic apoptotic pathway in YAC transgenic mouse model of Huntington's disease. *Mol Cell Neurosci* **25**, 469–479.

Zeron MM, Hansson O, Chen N, Wellington CL, Leavitt BR, Brundin P, Hayden MR & Raymond LA (2002). Increased sensitivity to *N*-methyl-D-aspartate receptor-mediated excitotoxicity in a mouse model of Huntington's disease. *Neuron* **33**, 849–860.

Zucker RS (1973). Changes in the statistics of transmitter release during facilitation. *J Physiol* **229**, 787–810.

Zucker RS (2005). Minis: whence and wherefore? *Neuron* **45**, 482–484.

Acknowledgements

We would like to thank Dr G. Awatramani, Professor T. Murphy, Dr C. Cepeda and Professor M. Levine for guidance, Professor M. Hayden for comments on the manuscript, Dr C. Brown for statistical advice and Ms T. Okbinoglu for excellent technical assistance. This work was supported by: the Canadian Institutes for Health Research (A.J.M. and L.A.R), the Michael Smith Foundation for Health Research (A.J.M. and L.A.R) and the Bluma Tischler Foundation (A.J.M.).